

## Viscoelastic and Electrical Transitions in Gelation of Electrically Conducting Polyaniline

Mari Tiitu,<sup>†</sup> Panu Hiekkataipale,<sup>†</sup> Juha Hartikainen,<sup>†</sup> Tapio Mäkelä,<sup>‡</sup> and Olli Ikkala<sup>\*,†</sup>

Department of Engineering Physics and Mathematics and Center for New Materials, Helsinki University of Technology, P.O. Box 2200, FIN-02015 HUT, Espoo, Finland, and VTT Electronics, Microelectronics, P.O. Box 110, FIN-02044 VTT, Finland

Received November 7, 2001; Revised Manuscript Received April 1, 2002

**ABSTRACT:** In an effort to study viscoelastic (vector) percolation and conductivity (scalar) percolation within a single system, we demonstrate a conducting polymer/solvent system, which upon gelation undergoes a viscoelastic transition, followed by a separate conductivity transition. Polyaniline doped by camphorsulfonic acid, i.e., PANI(CSA)<sub>0.5</sub>, shows three regimes in mixtures with *m*-cresol at a narrow concentration window of ca. 6.5–7.5 wt %. At small aging times, a viscous fluid (sol) is encountered with poor conductivity. Upon gelation, the system enters a state with elastic behavior but with poor conductivity. Further aging leads to conductivity percolation with ca. 4 orders of magnitude increase of conductivity. The scaling exponents for gelation are  $t \approx 2.0$ – $2.5$  for the equilibrium modulus  $G_0 \sim |\epsilon|^t$  and  $s \approx 1.0$ – $1.2$  for the zero shear rate viscosity  $\eta_0 \sim |\epsilon|^{-s}$  where  $\epsilon = (t - t_{\text{gel}})/t_{\text{gel}}$ . The present observations may also be relevant in applications to understand the homogeneity of solid films upon solvent evaporation: The early “trapped” junction zones in gelation can cause the previously observed granular structures in solid films, if the junction zones grow during the solvent evaporation. This may limit the available conductivity levels in solid films.

### Introduction

Molecules containing several chemically reactive sites allow irreversible gelation where space-filling networks are formed in a solvent background.<sup>1–4</sup> Gelation can be considered as a transition from a viscous fluid state (sol), which contains only finite branched clusters, to an elastic solid state (gel), which contains an infinite network. This brought gelation into the context of critical phenomena and percolation<sup>5–10</sup> and motivated studies to compare gelation and its scaling exponents with a large variety of phase transitions.

Related developments have taken place also in the case of reversible gelation where the junction zones of the network are formed due to noncovalent interactions, such as helical domains, microcrystalline bundles, hydrogen bonding, coordination, hydrophobic effect, or some other physical interactions.<sup>4,11–13</sup> It has, however, been pointed out<sup>14</sup> that the reversible gels may actually be more complicated as the aggregating units are fibrils, and the thermoreversible aggregates may not appropriately be described to be fractal-like, demanding other types of analysis.<sup>15</sup> Typically, the physical cross-links can be “opened” upon heating in systems involving organic solvents or cooling in systems involving aqueous solutions. Therefore, the sol–gel transition is reversible in this case. The literature describes numerous polymer/solvent systems where reversible gelation has been studied in detail, e.g., *a*-PS/CS<sub>2</sub>, PVC/plasticizers, and aqueous gelatin.<sup>4,11–14,16,17</sup> The transition manifests in dynamic rheology<sup>11,13,16–18</sup> with characteristic storage and loss moduli  $G' \ll G''$ ,  $G' \sim \omega^2$ ,  $G'' \sim \omega^1$  in the sol state and  $G' \gg G''$ ,  $G' \sim \omega^0$  in the gel state, implying transition from a viscous fluid to an elastic solid.

In the field of irreversible and reversible gelation, there have been considerable efforts to understand the phase transition and to analyze the critical exponents.<sup>6–10,14,19–26</sup> In the percolation model, the progress of the gelation is described by the relative distance from the critical point  $\epsilon = (p - p_c)/p_c$ , where the reaction coordinate  $p$  can be taken, e.g., the gelation time. Near the gel point, the static viscosity diverges as  $\eta_0 \sim |\epsilon|^{-s}$  for  $p < p_c$  and the static elastic modulus decreases as  $G_0 \sim |\epsilon|^t$  for  $p > p_c$ , which define the scaling exponents  $s$  and  $t$ .<sup>6–8,10,21–26</sup>

Experimentally, there have been numerous studies using different materials and experimental setups for gelation, and they render  $t \approx 1.8$ – $2.6$  and  $s \approx 0.7$ – $1.5$ .<sup>6–8,10,21–26</sup> The gel time  $t_g$  can be identified as the time where both moduli reach the same slope vs frequency, i.e.,  $G' \sim G'' \sim \omega^\Delta$ , which also defines the third scaling exponent  $\Delta$ . Typically  $\Delta = 0.67$ – $0.75$ .

Theoretically, the classical Flory–Stockmeyer mean-field description (see e.g. ref 3) renders  $t = 3$  and  $s = 0$ , i.e., does not suggest divergent viscosity. There have been early efforts to understand gelation in terms of electrical percolation using resistor networks where the gel point would correspond to the first conducting pathway across the sample upon adding resistors to lattice points.<sup>6</sup> They would suggest  $t = 1.94$  and  $s = 0.75$ , leading to  $\Delta = 0.72$ , based on the so-called hyperscaling relation  $\Delta = t/(t + s)$ .<sup>10</sup> However, the electrical percolation is a scalar percolation, and it later turned out that it is more appropriate to describe gelation using a vector percolation.<sup>10,19</sup> In such a rigidity percolation, the suggested values depend on whether bond-bending forces are included,  $t = 3.75$ , not allowed (i.e., considering only so-called central forces),  $t = 2.1$ , or whether the polymeric entropy is specifically taken into account,  $t = 2.64$ .<sup>27</sup> Static and dynamic elastic percolation suggests

<sup>†</sup> Helsinki University of Technology.

<sup>‡</sup> VTT Electronics.

$s = 0.6-0.9$  or  $s = 1.3-1.5$ , respectively (for a comprehensive review, see ref 10).

The difference of the elastic and conductivity percolation is the starting point of the present work: We became interested in identifying systems where the (visco)elastic vector percolation and conductivity scalar percolation could be studied using a single system. A natural choice would be solutions of doped conjugated polymers.<sup>28</sup> They are characteristically (semi)rigid, approaching liquid crystalline polymers, and therefore, it is nontrivial to achieve appreciable solubility in solvents due to strong aggregation tendency. In selected systems, thermoreversible gelation based on rigid or rodlike polymers have been studied in detail already early, e.g., helical polybenzylglutamate (for a review, see ref 29) and selected polyimides.<sup>30</sup> In conjugated polymers, gelation has usually been regarded as an obstacle to achieve high-quality aggregate-free solutions to prepare well-defined solution cast films, e.g., for molecular electronics. Therefore, gel inhibitors are sometimes used.<sup>31</sup> On the other hand, well-defined 3-dimensional gels based on *undoped*, i.e., nonconducting, poly(alkylthiophene)s have recently been studied<sup>32</sup> as well as corresponding reversible gels.<sup>33</sup> They may be doped afterward for conductivity if required. In the context of *doped* conjugated polymers, we introduced a conducting reversible gel based on dilute solution of polyaniline (PANI) dissolved in dodecylbenzenesulfonic acid.<sup>34</sup> Such materials show a viscous fluid state with poor conductivity at high temperatures and elastic behavior with improved conductivity upon cooling. Unfortunately, the high acidity and hygroscopicity prevented detailed rheological studied of such systems. The concept was extended to other sulfonic acids.<sup>35</sup>

Here we report our efforts based on PANI doped by camphorsulfonic acid (CSA) in *m*-cresol solvent. The materials are among the most studied in the field of conducting polymers to allow highly conducting solid films upon solvent evaporation<sup>36</sup> or liquid crystalline solutions at very high concentrations.<sup>37</sup> In contrast to the previous work, we focus on the intermediate concentrations and their long-term properties based on dynamic rheology and ac impedance. It turns out that material undergoes gelation and a separate conductivity transition upon aging time.

## Experimental Section

**Materials.** Polyaniline was synthesized using a conventional route.<sup>38</sup> The molecular weights are  $M_n = 25\,000$  g/mol and  $M_w = 140\,000$  g/mol (measured with GPC using the PS standards). PANI had been dried in a vacuum ( $10^{-2}$  mbar) at 60 °C for 1 day, and racemic CSA (Acros DL-10, purity 98%) was vacuum-dried at 60 °C for 1 day. Formic acid (Riedel de Haën) had the purity of at least 98%, and *m*-cresol (Acros) had the purity of 97%. The latter was dried using 3 Å molecular sieves.

**Sample Preparation.** PANI and CSA were mixed in formic acid using the ratio PANI:CSA 1:0.5 mol/mol (vs the PhN repeat units of PANI). The combined weight fraction of PANI + CSA was 2 wt % (i.e., 20 g), and consequently, the weight fraction of formic acid was 98 wt % (i.e., 980 g). It was mixed using a magnetic stirrer for 11 days and two times with Branson 450-D ultrasonic stirrer for about 10 h (see also ref 39 for dissolution concepts). The effect of the ultrasonic treatment on the molecular weight is discussed later. The sample container was cooled using circulated cold water in an external bath, which was in contact with the sample vessel. The temperature set at about 40 °C. Formic acid was evaporated on a hot plate at 60 °C. The resulting material, denoted

as PANI(CSA)<sub>0.5</sub> based on the nominal composition, was dried in a vacuum at 60 °C for 24 h. The sample was ground in a mortar and further dried in a vacuum at 60 °C for three additional days. Finally, the temperature was raised to 80 °C for 2 h in a vacuum to further remove the potential residuals of formic acid.

A small amount of PANI(CSA)<sub>0.5</sub> was dedoped with ammonia (0.3 wt % ammonia in water, 24 h) to find out whether the ultrasonic stirring had caused reduced molecular weight. Residual  $M_w$  was 100 000 g/mol (sulfuric acid solution measured with a Ubbelohde viscometer, which has been calibrated against GPC). It can be concluded that some scission of PANI chains had indeed taken place due to the ultrasonic treatment, probably leading to also broadened molecular weight distribution. However, we did not regard the degradation excessive, and definitely the scission does not promote the tendency for networking.

**Solubility in *m*-Cresol.** Several compositions are reported in this work: PANI(CSA)<sub>0.5</sub>/*m*-cresol 2.0/98.0, 5.0/95.0, 6.5/93.5, 7.0/93.0, 7.5/92.5, and 8.0/92.0 w/w. Higher concentrations underwent gelation immediately and those below ca. 6 wt % too slowly. Thus, the phenomena to be reported could be studied only at a narrow concentration window. PANI(CSA)<sub>0.5</sub> was slowly added into a bottle containing *m*-cresol, the bottle was immediately closed, and the mixtures, total of 6 g, were mixed for 15 min with a magnetic stirrer and for 40 min with an ultrasonic stirrer. At the end of the mixing, the temperatures reached temporarily ca. 50 °C due to ultrasonics. Immediately after the mixing, the samples were poured to the sample cells for rheological and conductivity measurements at the room temperature, and the measurements were promptly initiated. Within the resolution of optical microscopy, solubility was achieved without major insoluble particles.

Note a comment on the sample preparation: In a conventional method of preparation for molecular electronics, the sample solutions are finally filtered to remove the possibly insoluble particles (see e.g. ref 40). We were not willing to perform such a procedure, as it would have further "observed" definition of the initial time of the gelation measurement. In fact, it was the omission of the filtering step which suggested us to use the rather harsh dissolution concepts using ultrasonic treatment.

**Dynamic Rheology.** A strain-controlled Bohlin VOR rheometer was used with a coaxial cylindrical C14 sample cell: The measuring geometry consists of a fixed bob (inner cylinder of diameter 14 mm and cone angle 15°) located in a rotating cup (outer cylinder of diameter 15.4 mm). As it is known that absorbed water could cause premature gelation,<sup>41</sup> efforts were made to make the measurements under anhydrous conditions: As it turned out difficult to close the whole rheometer in a glovebox in an inert gas, we closed the sample chamber inside a box which had only a hole for the sample cell axis and provided constant nitrogen gas flow into the box. The applied strain varied between 0.039 and 0.25. Linearity was checked in the beginning of the experiment.

**Impedance Spectroscopy.** The sample was sealed in a 2 mL glass bottle containing two platinum electrode strips of widths 5 mm and lengths 27 mm and having mutual separation of ca. 3 mm. An argon atmosphere was used when sealing the sample, and epoxy glue was applied over the cap to prevent water absorbing to the sample. The electrodes of the bottle were attached directly to the terminals of the HP 4192A LF impedance analyzer. The ac impedance was measured between 10 and 10<sup>7</sup> Hz.

## Results

**Viscoelastic Transition.** Figure 1 shows the viscoelastic behavior for PANI(CSA)<sub>0.5</sub>/*m*-cresol 6.5/93.5 w/w at different aging times upon mixing PANI(CSA)<sub>0.5</sub> with *m*-cresol. At the aging time 3 h,  $G' \propto \omega^{1.4}$ ,  $G'' \propto \omega^1$ , and  $G' \ll G''$ , which suggests a viscous fluid. The exponent of  $G'$  is slightly smaller than that of ideal solutions  $G' \propto \omega^2$ , which may, in part, be due to the time

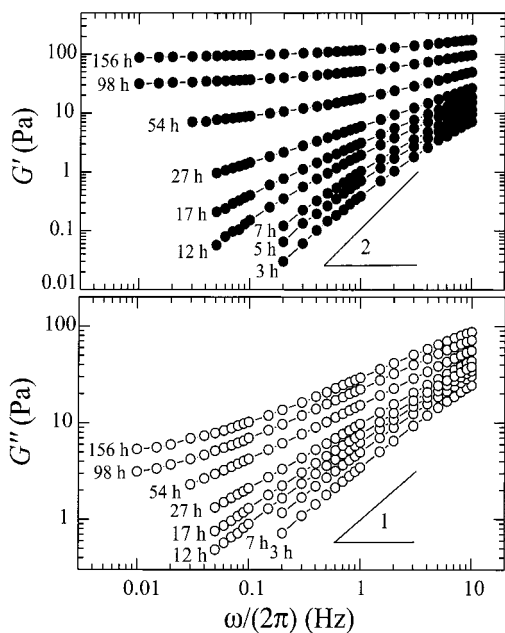


**Figure 1.** Dynamic rheological storage and loss moduli for PANI(CSA)<sub>0.5</sub>/m-cresol 6.5/93.5 w/w at different aging times after mixing.

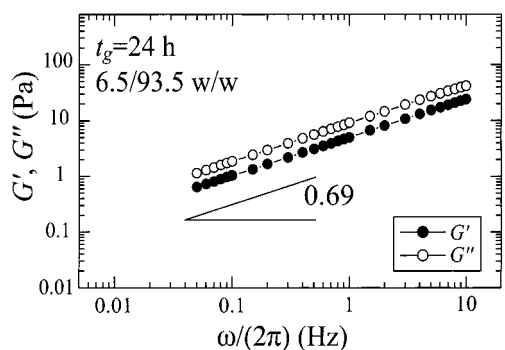


**Figure 2.** Dynamic rheological storage and loss moduli for PANI(CSA)<sub>0.5</sub>/m-cresol 6.5/93.5 w/w at the gel time.

elapsed to load the sample into the rheometer and to perform the first measurement. After  $t_g = 24$  h the slopes of  $G'$  and  $G''$  vs  $\omega$  become equal (slope  $\Delta = 0.69$ ) (Figure 2), which specifies the gel time  $t_g$ . After 156 h,  $G'$  has become essentially independent of  $\omega$  whereas  $G'' \propto \omega^{0.4}$  and  $G' \gg G''$ . Therefore, Figure 1 demonstrates a transition from a viscous fluid to an elastic solid, which suggests a network formation.

Higher PANI(CSA)<sub>0.5</sub> concentrations in *m*-cresol behave qualitatively similarly, however, showing shorter gelation times  $t_g$  (see Figure 3 and Table 1). Note that the gelation time for concentration 7.5/92.5 w/w was only 7.8 h, and in the case of 8/92 w/w gelation took place already before the sample could be loaded into the rheometer. The relative error in the gel time determination becomes larger for the higher concentrations, i.e., for the short gel times.

The simplest model for the gelation time  $t_g$ <sup>42,43</sup> is given by

$$\frac{1}{t_g} = kC^n$$

where  $k$  is the rate constant,  $C$  is the polymer concentration, and  $n$  is the average number of polymer chains participating in the formation of a junction zones. Figure

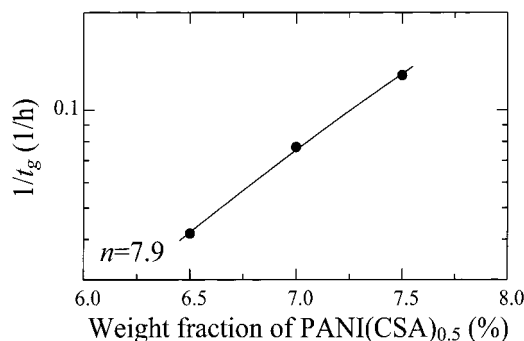


**Figure 3.** Reciprocal of the gelation time vs weight fraction of PANI(CSA)<sub>0.5</sub> in *m*-cresol.

**Table 1. Viscoelastic Scaling Exponents Observed for PANI(CSA)<sub>0.5</sub>/m-Cresol Observed during Gelation upon Aging<sup>a</sup>**

PANI(CSA) <sub>0.5</sub> / m-cresol (w/w)	gel time $t_g$ (h)	$t$	$s$	$\Delta = t/(s+t)$ from $s$ and $t$	$\Delta$ from $G'$ $\sim \omega^\Delta$
6.5/93.5	24	2.24	1.02	0.69	0.69
7.0/93.0	13	2.03	0.95	0.68	0.70
7.5/92.5	7.8	2.52	1.2	0.68	0.68
8.0/92.0	"instant"				

<sup>a</sup>  $G_0 \sim |\epsilon|^t$  and  $\eta_0 \sim |\epsilon|^{-s}$ . In the concentration 8.0/92.0, the gelation was too rapid to be evaluated using the present setup (marked as "instant").

3 suggests  $n \approx 8$ . For comparison,  $n$  has been found to be  $4.5 \pm 0.5$  and  $12.5 \pm 0.9$  for  $\iota$ - and  $\kappa$ -carrageenan, respectively.<sup>43</sup> Note, however, that the above model has not unambiguously been accepted.<sup>43</sup> An important side result is that the model crudely allows extrapolating the solution stability for dilute solutions, such as 1.0 wt %, which would indicate that they may be practically stable for years. However, in casting solid films, high concentrations are intermediate states, in which case network formation is unavoidably quick. Such behavior could be of importance to understand the suggested inhomogeneous or "granular" structure of the solid films (see later).

To determine the viscoelastic scaling exponents, master curves are next compiled, which combine the rheological data of a given sample at different aging times. Our approach follows that presented in ref 25 (see also ref 24): The average relaxation time is given by

$$\langle \tau \rangle \sim \int_0^\infty G(t) dt \sim |\epsilon|^{-s}$$

and the longest relaxation time

$$\tau_z = \frac{\int_0^\infty tG(t) dt}{\int_0^\infty G(t) dt} \sim |\epsilon|^{-s-t}$$

where  $G(t)$  is the shear relaxation modulus.<sup>44</sup> As discussed previously,  $\omega$  can be scaled by the longest relaxation time  $\tau_z$ , and therefore the "horizontal" shift factor scales as  $a_h \sim |\epsilon|^{-s-t}$ . On the other hand,  $G(\omega)$  can be scaled by the equilibrium modulus  $G_0 \sim 1/J_e^0$ , using the steady-state creep compliance. As  $\tau_z \sim \eta_0 J_e^0$  and  $\eta_0 \sim \langle \tau \rangle$ , we conclude  $1/J_e^0 \sim |\epsilon|^t$ , and  $G'$  and  $G''$  should be scaled by the "vertical" shift factor  $a_v \sim |\epsilon|^t$ .<sup>25</sup> Accordingly, Figure 4 shows data concerning PANI(CSA)<sub>0.5</sub>/m-cresol 6.5/93.5 w/w at different aging times, as combined to master curves  $a_v G'$  and  $a_v G''$  as a function



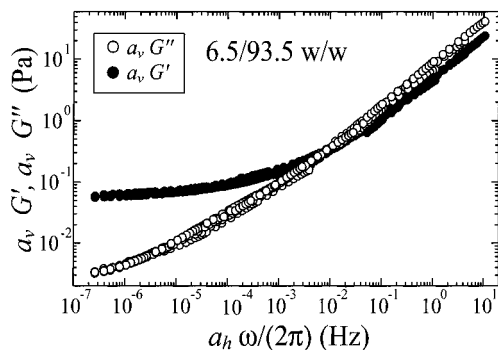


**Figure 4.** Viscoelastic master curves for PANI(CSA)<sub>0.5</sub>/*m*-cresol 6.5/93.5 w/w beyond the gel point. The master curves contain aging times 26.7, 31.5, 36, 45, 54, 62.7, 71.5, 98, 130, 156.5, and 171 h. The gel time  $t_g = 24$  h.

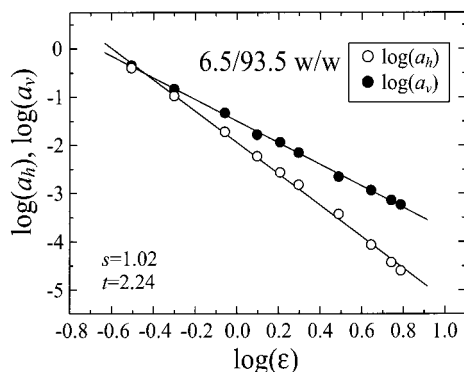


**Figure 5.** Shift factors used to compile the master curve for PANI(CSA)<sub>0.5</sub>/*m*-cresol 6.5/93.5 w/w (Figure 4).

of the scaled frequency  $a_h\omega$ . Figure 5 shows the corresponding shift factors  $a_v$  and  $a_h$  as a function of  $\epsilon$ . First of all, one can conclude that common shift factors can be found which combine data of different aging times to a single master curve. Second, the shift factors behave smoothly and linearly vs  $\epsilon$  in double-logarithmic plots (Figure 5). Table 1 shows the observed exponents where  $-t$  and  $-t-s$  are obtained from the slopes of  $a_v$  and  $a_h$ . The scaling exponent for the moduli fall in the range  $t \approx 2-2.5$ , depending on the concentration. Note that  $t \approx 3.75$  is suggested in rigidity percolation if one assumes that, in addition to central forces acting only along the bonds, there are also bond-bending constraints that limit bending around the cross-link sites, leading to increased stiffness. Removing the bond-bending constraints renders  $t \approx 2.1$  in the central-force case. However, if one includes also the polymeric entropy, the value  $t \approx 2.64$ . In agreement,  $t \approx 2.7$  has been observed for a chemical gel, involving polyoxypropylene with chemically reactive silyl end groups.<sup>26</sup> By contrast,  $t \approx 1.94$  has been obtained for pectin, effectively cross-linked by  $\text{Ca}^{2+}$  complexation, which almost totally coincides with the value suggested for scalar percolation involving resistors.<sup>24</sup> Our values are slightly higher, in broad agreement with elastic rigidity percolation.

Considering the other exponents, there seems to be an agreement that  $\Delta \approx 0.70$ . In the present case, we can extract its value by two ways: first, by using the slopes of  $G$  and  $G'$  vs  $\omega$  at the gel point (Figure 2), and second, by using the hyperscaling  $\Delta = t/(t+s)$ . Both methods agree and render  $\Delta \approx 0.68-0.70$  (see Table 1). Finally, the present value  $s \approx 1.0$  falls near the static elastic percolative network values, as suggested on the basis of the Zimm model.<sup>10</sup>

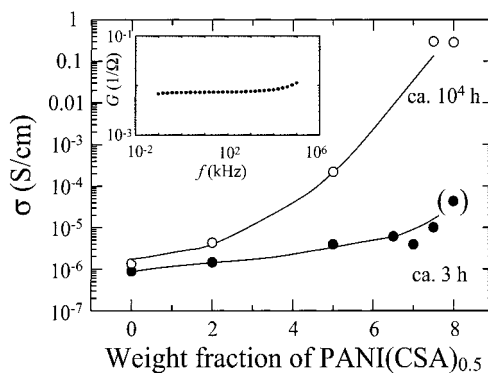


**Figure 6.** Electrical dc conductivity  $\sigma$  of PANI(CSA)<sub>0.5</sub>/*m*-cresol vs the weight fraction of PANI(CSA)<sub>0.5</sub> after aging times 3 and 10 000 h. The point corresponding to 8 wt % is already beyond the gel point and marked in parentheses. The inset shows an example of conductance vs frequency of the sample 6.5/93.5 w/w after aging of 1500 h.

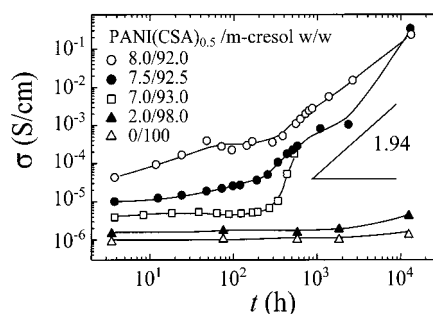


**Figure 7.** Electrical dc conductivity  $\sigma$  of PANI(CSA)<sub>0.5</sub>/*m*-cresol vs time at different weight fractions.

**Conductivity Transition.** The ac impedances were measured using the blocked electrode configuration involving two parallel Pt plates. Cole–Cole plots for the real and imaginary parts of the impedances were plotted as a function of frequency. In comparison to the ideal semicircle behavior, as explained by a parallel resistor and capacitor, the plots became progressively “flattened”, potentially suggesting that broadened distribution of relaxation times develop during the aging. However, as we were unable to perform unambiguous quantitative analysis, we omit such plots here. As a function of frequency, the conductances showed a characteristic plateau near 1 kHz (see the inset of Figure 6), which allowed extrapolation to zero frequency, to render dc resistances. *m*-Cresol shows a conductivity of the order of  $10^{-6}$  S/cm, probably due to residual impurities and some almost inevitably absorbed water, despite the inert atmosphere conditions. The initial dc conductivities of PANI(CSA)<sub>0.5</sub>/*m*-cresol mixtures are shown at the aging times of ca. 3 h (Figure 6). Note that they represent the viscous sol state except PANI(CSA)<sub>0.5</sub>/*m*-cresol 8.0/92.0, which was already beyond the gel point. There is only a slight increase in the conductivity as a function of PANI(CSA)<sub>0.5</sub> concentration, and no distinct percolation was evident. Figure 7 shows how the dc conductivity develops as a function of time. At lower concentrations, such as 2/98 w/w, the conductivity remains at a low level up to 10 000 h. However, for example, the sample 7.5/92.5 w/w shows increase of conductivity from ca.  $10^{-5}$  to in excess of 0.1 S/cm, i.e., 4 orders of magnitude. Interestingly, the increase takes place after hundreds of hours, i.e., much later than the viscoelastic gel point, i.e.,  $t_g \approx 7.8$  h for 7.5/92.5 w/w.

In conclusion, a percolation-like transition was observed also in conductivity, but astonishingly the critical times seem to be orders of magnitude longer than in the viscoelastic transition. Therefore, the most important finding of the present paper is that the viscoelastic and electrical transition are sequential and distinct.

More quantitative analysis of the electrical percolation could not be made due to the scatter of the data. The very long required times (more than a year) do not encourage more repetitions. In the electrical (scalar) percolation one expects the scaling  $\sigma \sim |\epsilon|^t$  with  $t \approx 1.94$ .<sup>6,9</sup> In passing, the slope 1.94 vs  $t$  has also been indicated in Figure 7. Even when the scatter does not allow unambiguous conclusions on the scaling exponent, one may conclude that there may be no evident conflict to value  $t \approx 1.94$ . Note also (Figure 6) that the conductivities after aging of 10 000 h indicate lower percolation threshold vs PANI(CSA)<sub>0.5</sub> concentration than prior to gelation and conductivity transition.

## Discussion

The shown rheological and conductivity experiments are different in the sense that in the first ones the sample is sheared whereas in the latter ones the sample is under a quiescent condition. Previously, it has been observed that rheological history can have essential effects on the reversible gelation.<sup>45</sup> To check whether keeping the samples in a quiescent condition would extend the gel time to the ones observed in the conductivity transitions, we performed a modification of "a falling ball experiment".<sup>46</sup> New samples were prepared where PANI(CSA)<sub>0.5</sub> was poured in 10 mL glass bottles containing *m*-cresol (dried by 3 Å molecular sieves, as before) and immediately sealed with a cap, to render samples with concentrations 5/95 and 8/92 w/w. The total weight of the samples including *m*-cresol was 6 g. The samples were mixed as before, i.e., 15 min using a magnetic stirrer and 40 min using ultrasound in which case the sonicator tip was punched through the rubber caps of the glass bottles. Immediately after the mixing, the glass bottles were resealed with fresh caps under an argon atmosphere. The closed glass bottles contained steel balls and by periodically turning the glass bottles it could be crudely determined whether the sample was viscous fluid or elastic solid. PANI(CSA)<sub>0.5</sub>/*m*-cresol 5.0/95.0 w/w gelled during 8 days, whereas PANI(CSA)<sub>0.5</sub>/*m*-cresol 8.0/92.0 gelled in less than 1 day using this method. It can be concluded that the shear history may not be the main reason for the shorter time observed in the viscoelastic transition. The falling ball test allowed to check also another aspect: The potentially absorbed water may cause gelation in extremely dilute PANI solutions<sup>41</sup> as well as in other rigid-rod solutions.<sup>47</sup> The qualitatively similar gelation times in the rheological and falling ball experiments suggest that the viscoelastic gelation may not be caused simply by progressively absorbed water during the rheological measurements despite the inert gas conditions.

We will next address the junction zones. Upon the viscoelastic transition (gelation), junction zones are developed that allow sufficient chain-to-chain fixation to render elasticity. However, only upon prolonged aging time does the conductivity transition take place. We will present two hypotheses, neither of which can be proven at the present time: In the first hypothesis, the junction zones grow upon aging, and in the conductivity transition the junction zones pass a critical size to allow

improved hopping conductivity from one chain to another. The other hypothesis is that the order within the junction zones becomes gradually improved ("annealing"), for example, due to slow formation of (micro)-crystallinity. Only when the crystallites reach a critical size does the chain-to-chain hopping conductivity become significant, which would take several hundreds hours.

We next studied the possible crystallization within the junction zones. As the total volume fraction of such crystallites is expected to be very small, we used intense synchrotron radiation at ESRF (Grenoble) to obtain wide-angle X-ray scattering data. However, no crystallinity was resolved, and the structure of the junction zones remains so far open. There is, however, indirect evidence why such crystallization might still take place. The solid films of PANI(CSA)<sub>0.5</sub>, obtained upon evaporation of *m*-cresol, are typically granular, containing crystalline and amorphous domains.<sup>48–50</sup> The granularity may be connected to the gelation: Suppose that a film is cast using dilute solution of PANI(CSA)<sub>0.5</sub>, which is initially a viscous solution. As *m*-cresol is evaporated, and the concentration increases, gelation is initiated, leading to the formation of junction zones. Suppose that the junction zones contain crystallites. As the evaporation of *m*-cresol progresses, the crystallization is observed to increase,<sup>51</sup> suggesting that crystallites would grow until the coiled linking chains that connect the zones topologically prevent further growth. Therefore, the model would naturally explain that the observed granular properties of films have been developed from the trapped junction zones, which ultimately may limit the conductivity levels obtainable.

Finally, the possible thermoreversibility is considered: The present gels could not be "melted" upon slight heating, i.e., before excessive evaporation of *m*-cresol took place. However, PANI(CSA)<sub>0.5</sub> mixed with resorcinol (where the CH<sub>3</sub> of *m*-cresol is replaced with a OH-group, which allows improved attraction due to two hydrogen-bonding groups) causes a cocrystalline molecular complex, which melts at elevated temperatures near 200 °C<sup>52</sup> (see also ref 53). This suggests that even in the present case the potential crystallites would melt upon heating to near 200 °C, which, however, is not feasible due to the boiling point of *m*-cresol. Therefore, we suggest that the gels may in principle be thermoreversible; however, in practice the reversibility may be suppressed due to the evaporation of the solvent at the required high temperature.

## Conclusions

We have studied PANI(CSA)<sub>0.5</sub> dissolved in *m*-cresol. Using dynamic rheology and ac impedance, we show three different regimes of PANI(CSA)<sub>0.5</sub> in *m*-cresol, each having characteristic viscoelastic and conductivity behavior. A sol state which behaves as a viscous fluid and has poor conductivity is obtained immediately after mixing PANI(CSA)<sub>0.5</sub> and *m*-cresol, taken that the concentration of PANI(CSA)<sub>0.5</sub> is in the range ca. 6.5–7.5 wt %. As the aggregation proceeds, viscoelastic transition (gelation) takes place, suggesting that chain-to-chain junction zones develop. In a gel, the junction zones can be sufficient "sticky" to allow elastic behavior but do not support electrical hopping from one chain to another, leading to poor conductivity. The third regime is entered upon prolonged aging where a separate electrical transition evolves. It is postulated that the

three states are inherent intermediates to explain the granular morphology in thin films of coiled conducting polymers, such as polyaniline and polythiophenes.

**Acknowledgment.** We acknowledge discussions and collaboration with J. Ruokolainen, P. J. Passiniemi, M. Torkkeli, R. Serimaa, V. Honkimäki, H. Kosonen, G. ten Brinke, H. Tenhu, K. Kontturi, and S. Valkama. We are grateful to P. Oittinen for permission to use the rheometer of her laboratory. Grenoble Synchrotron facility (ESFR) is acknowledged for the WAXS measurements. National Technology Agency (Finland) and Academy of Finland (Graduate School for Nanotechnology) are acknowledged for grants. PANIPOL Ltd. is thanked for polyaniline.

## References and Notes

- (1) Flory, P. J. *J. Am. Chem. Soc.* **1941**, *63*, 3083.
- (2) Stockmayer, W. H. *J. Chem. Phys.* **1943**, *11*, 45.
- (3) *Physical Properties of Polymeric Gels*, Cohen Addad, J. P., Ed.; John Wiley & Sons: New York, 1996.
- (4) *Chemical and Physical Networks: Formation and Control of Properties*; te Nijenhuis, K., Mijs, W. S., Eds.; John Wiley & Sons: Chichester, 1998; Vol. 1.
- (5) Gordon, M. *Faraday Discuss.* **1974**, *57*, 1.
- (6) de Gennes, P.-G. *Scaling Concepts in Polymer Physics*; Cornell University Press: Ithaca, NY, 1979.
- (7) Stauffer, D. *Phys. Rep.* **1979**, *54*, 1.
- (8) Stauffer, D.; Coniglio, A.; Adam, M. *Adv. Polym. Sci.* **1982**, *44*, 103.
- (9) Bunde, A.; Havlin, S. *Fractals and Disordered Systems*, 2nd ed.; Springer: Berlin, 1996.
- (10) Sahimi, M. *Phys. Rep.* **1998**, *306*, 213.
- (11) *Physical Networks: Polymers and Gels*; Burchard, W., Ross-Murphy, S. B., Eds.; Elsevier: London, 1990.
- (12) Guenet, J.-M. *Thermoreversible Gelation of Polymers and Biopolymers*; Academic Press: London, 1992.
- (13) te Nijenhuis, K. *Adv. Polym. Sci.* **1997**, *130*, 1.
- (14) Guenet, J.-M. *J. Rheol. (N.Y.)* **2000**, *44*, 947.
- (15) Jones, J. L.; Marques, C. M. *J. Phys. (Paris)* **1990**, *51*, 1113.
- (16) Li, L.; Aoki, Y. *Macromolecules* **1997**, *30*, 7835.
- (17) Li, L.; Aoki, Y. *Macromolecules* **1998**, *31*, 740.
- (18) Kavanagh, G. M.; Ross-Murphy, S. B. *Prog. Polym. Sci.* **1998**, *23*, 533.
- (19) Feng, S.; Sen, P. N. *Phys. Rev. Lett.* **1984**, *52*, 216.
- (20) Chambon, F.; Petrovic, Z. S.; MacKnight, W. J.; Winter, H. H. *Macromolecules* **1986**, *19*, 2146.
- (21) Durand, D.; Adam, M.; Luck, J. M. *Europhys. Lett.* **1987**, *3*, 297.
- (22) Martin, J. E.; Adolf, D.; Wilcoxon, J. P. *Phys. Rev. Lett.* **1988**, *61*, 2620.
- (23) te Nijenhuis, K.; Winter, H. H. *Macromolecules* **1989**, *22*, 411.
- (24) Axelos, M. A. V.; Kolb, M. *Phys. Rev. Lett.* **1990**, *64*, 1457.
- (25) Hodgson, D. F.; Amis, E. J. *Macromolecules* **1990**, *23*, 2512.
- (26) Takahashi, M.; Yokoyama, K.; Masuda, T.; Takigawa, T. *J. Chem. Phys.* **1994**, *101*, 798.
- (27) Daoud, M.; Coniglio, A. *J. Phys. A* **1981**, *14*, L301.
- (28) *Handbook of Conducting Polymers*, 2nd ed.; Skotheim, T. A., Elsenbaumer, R. L., Reynolds, J. R., Eds.; Marcel Dekker: New York, 1998.
- (29) Greiner, A.; Rochefort, W. E. In *Mechanical and Thermophysical Properties of Polymer Liquid Crystals*, 1st ed.; Brostow, W., Ed.; Chapman & Hall: London, 1998.
- (30) Kyu, T.; Yang, J.-C.; Cheng, S. Z. D.; Hsu, S. L. C.; Harris, F. W. *Macromolecules* **1994**, *27*, 1861.
- (31) Yang, D.; Adams, P. N.; Mattes, B. R. *Synth. Met.* **2001**, *119*, 301.
- (32) Bras, J.; Guillerez, S.; Pépin-Donat, B. *Chem. Mater.* **2000**, *12*, 2372.
- (33) Malik, S.; Jana, T.; Nandi, A. K. *Macromolecules* **2001**, *34*, 275.
- (34) Vikki, T.; Ruokolainen, J.; Ikkala, O. T.; Passiniemi, P.; Isotalo, H.; Torkkeli, M.; Serimaa, R. *Macromolecules* **1997**, *30*, 4046.
- (35) Jana, T.; Nandi, A. K. *Langmuir* **2000**, *16*, 3141.
- (36) Cao, Y.; Smith, P.; Heeger, A. J. *Synth. Met.* **1992**, *48*, 91.
- (37) Cao, Y.; Smith, P. *Polymer* **1993**, *34*, 3139.
- (38) Cao, Y.; Andreatta, A.; Heeger, A. J.; Smith, P. *Polymer* **1989**, *30*, 2305.
- (39) Cao, Y.; Smith, P.; Heeger, A. J. WO 92/22911, 1992.
- (40) Kosonen, H.; Ruokolainen, J.; Knaapila, M.; Torkkeli, M.; Jokela, K.; Serimaa, R.; ten Brinke, G.; Bras, W.; Monkman, A. P.; Ikkala, O. *Macromolecules* **2000**, *33*, 8671.
- (41) Gettinger, C. L.; Heeger, A. J.; Pine, D. J.; Cao, Y. *Synth. Met.* **1995**, *74*, 81.
- (42) Oakenfull, D. *J. Food Sci.* **1984**, *49*, 1103.
- (43) Ross-Murphy, S. B. *Food Polym., Gels, Colloids* **1991**, 357.
- (44) Ferry, J. D. *Viscoelastic Properties of Polymers*, 3rd ed.; John Wiley & Sons: New York, 1980.
- (45) Narh, K. A.; Barham, P. J.; Keller, A. *Macromolecules* **1982**, *15*, 464.
- (46) Tan, H. M.; Chang, B. H.; Baer, E.; Hiltner, A. *Eur. Polym. J.* **1983**, *19*, 1021.
- (47) Russo, P. S.; Siripanyo, S.; Saunders, M. J.; Karasz, F. E. *Macromolecules* **1986**, *19*, 2856.
- (48) Pouget, J. P.; Oblakowski, Z.; Nogami, Y.; Albouy, P. A.; Laridjani, M.; Oh, E. J.; Min, Y.; MacDiarmid, A. G.; Tsukamoto, J.; Ishiguro, T.; Epstein, A. J. *Synth. Met.* **1994**, *65*, 131.
- (49) Epstein, A. J.; Joo, J.; Kohlman, R. S.; Du, G.; MacDiarmid, A. G.; Oh, E. J.; Min, Y.; Tsukamoto, J.; Kaneko, H.; Pouget, J. P. *Synth. Met.* **1994**, *65*, 149.
- (50) Travers, J. P.; Sixou, B.; Berner, D.; Wolter, A.; Rannou, P.; Beau, B.; Pépin-Donat, B.; Barthet, C.; Guglielmi, M.; Mermilliod, N.; Gilles, B.; Djurado, D.; Attias, A. J.; Vautrin, M. *Synth. Met.* **1999**, *101*, 359.
- (51) Österholm, H.; Ikkala, O. Unpublished results, 1993.
- (52) Vikki, T.; Pietilä, L.-O.; Österholm, H.; Ahjopalo, L.; Takala, A.; Toivo, A.; Levon, K.; Passiniemi, P.; Ikkala, O. *Macromolecules* **1996**, *29*, 2945.
- (53) Ikkala, O. T.; Pietilä, L.-O.; Ahjopalo, L.; Österholm, H.; Passiniemi, P. *J. Chem. Phys.* **1995**, *103*, 9855.

MA011943Z